Extended Abstracts of the 2007 International Conference on Solid State Devices and Materials, Tsukuba, 2007, pp. 44-45

B-2-2

Influences of Elastic and Inelastic Scatterings on Ballistic Transport in MOSFETs

Hideaki Tsuchiya[1] and Shin-ichi Takagi[2,3]

[1]Kobe University, Graduate School of Engineering
1-1, Rokko-dai, Nada-ku, Kobe 657-8501, Japan
Phone & Fax (common): +81-78-803-6082 E-mail: tsuchiya@eedept.kobe-u.ac.jp

[2]MIRAI-ASRC, AIST Tsukuba West 7, 16-1, Onogawa, Tsukuba 305-8569, Japan

[3]The University of Tokyo, Graduate School of Frontier Science
7-3-1, Hongo, Bunkyo-ku, Tokyo 113-8656, Japan

1. Introduction

Si-MOSFETs have been scaled down to a sub-10nm channel length [1], and a ballistic or quasi-ballistic transport is highly expected. Pioneering research on the ballistic transport in Si-MOSFETs has been performed by K. Natori, and he proposed that the elastic scattering degrades a ballisticity, while the inelastic scattering involving energy relaxation improves the ballisticity in contrast [2,3].

We examine in this paper the Natori's prediction using actual MOSFET structures based on a quantum-corrected Monte Carlo (QCMC) device simulator [4]. As a result, we found that the energy relaxation process in a channel indeed encourages the ballistic transport if the channel length is scaled down to the 10nm-scale, however, the mechanism is not so simple because the channel potential is fluctuated due to electric charges accumulated within the channel.

2. $\hbar\omega$–Layer Theory

First, we study a backscattering region where the carrier scattering reduces the drain current. Fig. 1 shows some characteristic aspects of scattering effects. According to Natori [2,3], carriers are injected from source to channel with kinetic energy of the order of thermal energy kT, and they suffer elastic and inelastic scatterings in the channel. Some carriers suffer the energy relaxation (ER) due to the inelastic optical phonon emission, which lose a few multiples of kT (61meV for Si) and have little chance to return to source, and are eventually absorbed into drain. Accordingly, the backscattering region is determined by a position where the potential decreases by the optical phonon energy of 61meV. We refer to this region as $\hbar\omega$–layer. This is analogous to the kT-layer discussed by Lundstrom [5], except that the length $L_{\hbar\omega}$ is controlled by the optical phonon energy.

A backscattering coefficient R is calculated by using $R = L_{\hbar\omega} / (L_{\hbar\omega} + \lambda^{\mathrm{back}}) \cdots (1)$ [5], where λ^{back} is a mean free path for backscattering in $L_{\hbar\omega}$. Fig. 2 shows the L_{ch} dependences of $L_{\hbar\omega}$, λ^{back} and R computed for double-gate MOSFETs with ultrathin ($T_{\mathrm{Si}} = 3$ nm) and undoped channels. It is found that the $\hbar\omega$–layer theory based on the ER principle agrees better than the kT-layer theory with the advanced QCMC approach [4] and the recent experimental results [6].

3. Influences of Elastic and Inelastic Scatterings

Next, we discuss the influences of each scattering mechanism. As show in Fig. 3, we performed four kinds of simulations for the double-gate MOSFET, which include (I) no scattering processes, (II) elastic processes, (III) elastic + inelastic emission processes and (IV) elastic + inelastic emission and absorption processes. Note that all scattering processes are always considered in the source and drain regions. The quantum effects are considered by using a quantum correction of potential [4], and the two-dimensional Poisson's equation is self-consistently solved. Fig. 4 shows the average electron velocity profiles computed for (a) $L_{\mathrm{ch}} = 10$ nm and (b) 30 nm. The lower figures summarize the source-end velocities v_s. It is found that the elastic and inelastic absorption processes decrease v_s for both channel lengths. (see (II) and (IV)). On the other hand, the inelastic emission processes have the opposite effect on v_s, depending on the channel length (see (III)). In short, the inelastic emission increases v_s for $L_{\mathrm{ch}} = 10$ nm, which coincides with the Natori's prediction, but it decreases v_s for $L_{\mathrm{ch}} = 30$ nm.

To understand the effects of such inelastic emission processes, we computed the variations in v_s and $L_{\hbar\omega}$ as a function of the left boundary of the ER region shown in Fig. 5, where the right boundary of the ER region is always set at the drain-end of channel. The results are shown in Fig. 6. For (a) $L_{\mathrm{ch}} = 10$ nm, v_s increases by including the inelastic emission processes as shown in Fig. 4 (a), but v_s is found to decrease once when the ER region approaches and slightly overlaps the $\hbar\omega$–layer. This is due to the increase in $L_{\hbar\omega}$ as shown in the dashed lines, which is owing to the potential uplift by the electric charges accumulated within the ER region. Next, for (b) $L_{\mathrm{ch}} = 30$ nm v_s slightly increases due to the ER region located close to the drain-end, and decreases significantly when the ER region approaches the $\hbar\omega$–layer. Consequently, the inelastic emission processes decrease v_s for $L_{\mathrm{ch}} = 30$ nm as shown in Fig. 4 (b). It should be also noted that the $\hbar\omega$–layer becomes shorter as the ER region overlaps a wide range of the $\hbar\omega$–layer. This is because the potential drops more quickly due to the increased resistance caused by the inelastic emission scattering.

4. Conclusion

It has been found that the inelastic scattering involving energy relaxation improves the ballistic transport in the 10nm-scale Si channels, while it degrades the ballisticity in the longer channels. Furthermore, since the backscattering to source is governed by the $\hbar\omega$–layer, a potential profile engineering at the source-end of channel is expected to be a strategy for improving the ballisticity.

Acknowledgements

This work is supported by NEDO/MIRAI project.

References [1] H. Wakabayashi et al., IEDM (2003) 989. [2] K. Natori, IEEE EDL-23 (2002) 655. [3] K. Natori, SSDM (2004) 728. [4] H. Tsuchiya et al., IEEE TED-53 (2006) 2965. [5] M. Lundstrom et al., IEEE TED-49 (2002) 133. [6] A. Tsuda et al, SSDM (2006) 352.

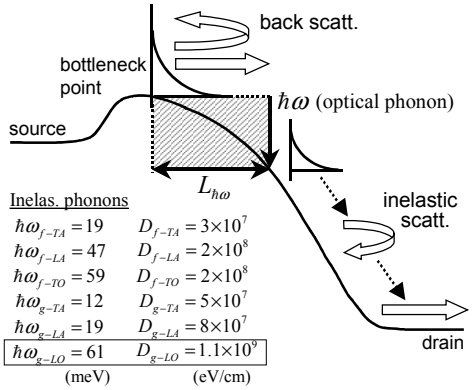

Fig. 1 Characteristic aspects of scattering effects on quasi-ballistic transport, and inelastic phonon energies $\hbar\omega$ and deformation potentials D. For Si, the *g-LO* type optical phonon with $\hbar\omega = 61$meV is found to be dominant. Note that all six kinds of inelastic phonons are considered in the present QCMC simulation.

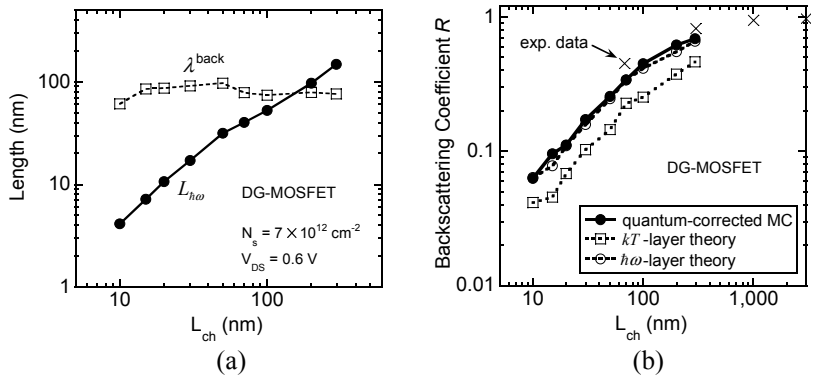

Fig. 2 (a)$L_{\hbar\omega}$ and λ^{back} as a function of L_{ch}, estimated by using the output data from the QCMC simulator. (b) denotes the backscattering coefficient R calculated by using the data of (a) and eq. (1) (open circles). The results for kT-layer theory are also plotted in the squares. Further, the results directly estimated from the QCMC simulator [4] and the experimental results [6] are plotted in the solid circles and the crosses, respectively.

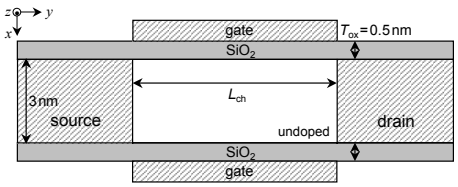

Scattering Processes Considered in Channel Region†

(I) no scattering (= ballistic channel)
(II) elastic processes
(III) elastic + inelastic emission processes
(IV) elastic + inelastic emission and absorption processes

(†Only phonon scatterings are considered.)

Fig. 3 Four kinds of simulations described above are performed for double-gate MOSFETs with ultrathin and undoped channels. In the source and drain regions, all scattering processes including plasmon scattering are always considered to activate the energy decay of hot electrons rapidly.

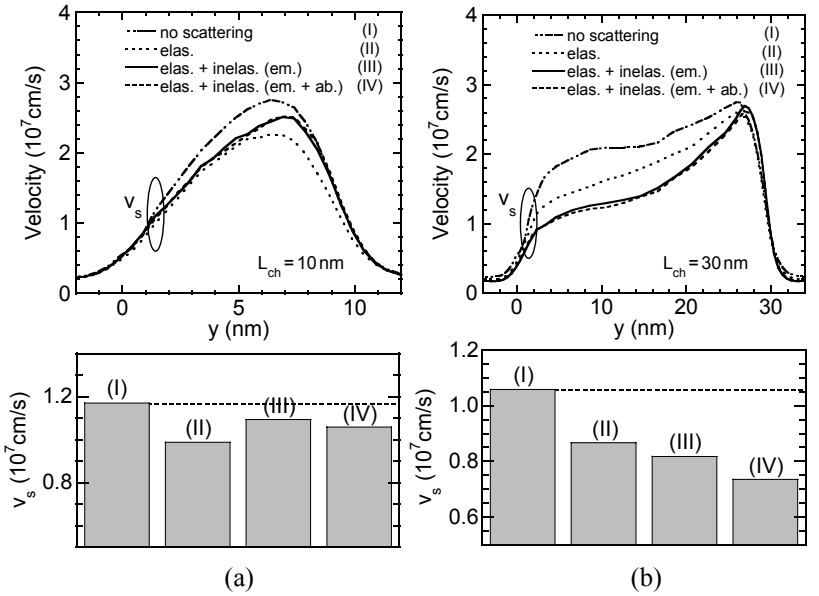

Fig. 4 Average electron velocity profiles computed for (a)L_{ch} = 10 nm and (b) 30 nm. The lower figures summarize the source-end velocities v_s for each condition.

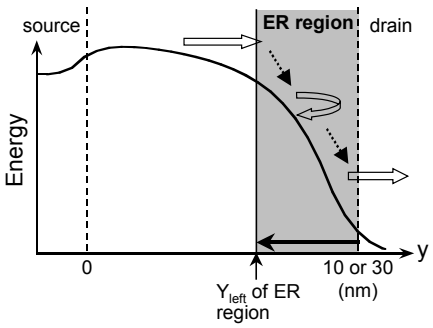

Fig. 5 Simulation model including the ER region, where the left boundary of the ER region is displaced from y = 10 or 30 nm to 0, while the right boundary is always set at the drain-end of channel.

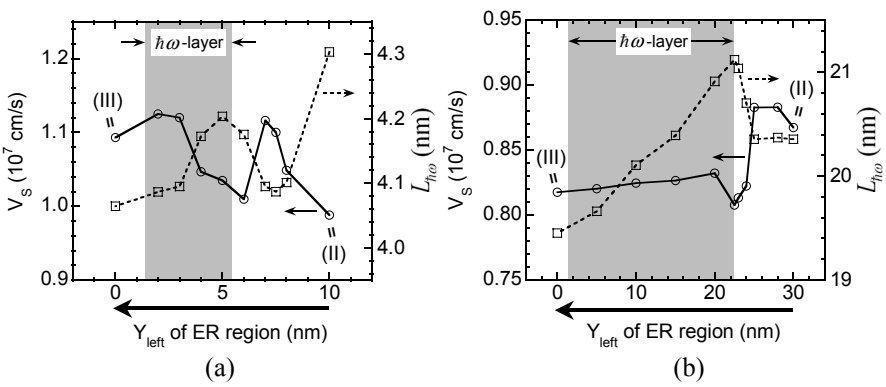

Fig. 6 Variations in v_s (circle) and $L_{\hbar\omega}$ (square) as a function of left boundary of the ER region shown in Fig. 5. (a) L_{ch} = 10 nm and (b) 30 nm. The shaded regions represent the $\hbar\omega$–layers for reference.